Available online at www.sciencedirect.com
ScienceDirect
Franklin Institute 00 (2023) 1–20
Franklin Institute

Linear Quadratic Integral Differential Game applied to the Real-time Control of a Quadrotor Experimental setup

Hadi Nobahari

Department of Aerospace Engineering Sharif University of Technology Tehran, Iran

Ali BaniAsad

Department of Aerospace Engineering Sharif University of Technology Tehran, Iran

Reza Pordal

Department of Aerospace Engineering Sharif University of Technology Tehran, Iran

Alireza Sharifi

Department of Aerospace Engineering Sharif University of Technology Tehran, Iran

Abstract

This research paper presents a novel approach to quadrotor attitude control that draws on differential game theory. The approach uses a linear quadratic Gaussian (LQG) controller with integral actions. Accurate attitude control is of utmost importance for safe and effective quadrotor flight, particularly in the presence of disturbances. To develop a dependable and effective control system, the motion equations with nonlinearity for the quadrotor's experimental setup are transformed into a continuous-time state-space model through linearization. The model parameters are identified through experimental data, and a two-player approach is employed to determine the attitude control commands. By mini-maximizing a quadratic set of criteria, which is the total of the outputs and disturbances weighted by the amount of control effort, one player minimizes the command while the other generates disturbances. The performance of the proposed approach is evaluated by comparing it to a linear quadratic regulator controller in level flight. The results demonstrate that the proposed approach effectively dissipates disturbances and outperforms linear quadratic regulator controllers, thereby contributing to the development of robust and effective attitude control systems for quadrotors.

Keywords:
Linear quadratic Gaussian controller, Differential game theory, Quadrotor, Continuous state-space model, 3-degree-of-freedom experimental platform, Attitude Control Optimization, Robust disturbance rejection.

1. Introduction

The investigation, strategic operations, optical sensing, entertainment, and farming are all used by quadrotors in today's society [1]. Various subsystems of the quadrotor control system are responsible for the quadrotor's perfor-

Email addresses: nobahari@sharif.edu (Hadi Nobahari), ali.baniasad@ae.sharif.edu (Ali BaniAsad), email address (Reza Pordal), alireza_sharifi@ae.sharif.edu (Alireza Sharifi)

mance, including attitude, altitude, and position. Maintaining the desired attitude outputs is essential for quadrotor attitude control, particularly in the presence of sudden disturbances. This can be achieved by controlling the rotor rotational speeds[2]. Consequently, there is a growing body of research focusing on the development of automatic control strategies for quadrotors to effectively manage disturbances and maintain desired attitudes. The quadrotor attitude is controlled by a Proportional Integral Derivative (PID) controller in [3, 4]. During disturbances, however, this controller has not effectively achieved the control obiectives. Model-based approaches to controller design are utilized to resolve this issue [5, 6]. Quadrotor attitude models and disturbances determine the direction of the best control commands using these controllers.

The literature has proposed numerous models-based controllers to provide a faster control algorithm when dealing with modeling errors and reducing disturbances. An intelligent controller, a robust controller, a nonlinear controller, and an optimal controller are some of these types of controllers.

Various control approaches based on intelligent logic, such as machine learning [7], evolutionary computation [8], iterative learning [9], reinforcement learning [10], and fuzzy logic [11], have been extensively employed for quadrotor attitude regulation. Numerous nonlinear control techniques have been proposed to regulate orientation angles of quadrotors, including Synergetic Control [12], Sliding Mode Control (SMC) [13], and Feedback Linearization (FBL) [14]. Robust control methods such as H_∞ [15, 16] and μ-synthesis [17] have also been utilized to stabilize the attitudes of quadrotors under conditions of extreme uncertainty and worst-case scenarios. Quadrotors have also been controlled using optimal controllers, such as the Linear Quadratic Gaussian (LQG) [18] and the Linear Quadratic Regulator (LQR) [19]. These controllers minimize a quadratic criterion by considering both regulation performance and control effort to provide optimal feedback gains. The Linear Quadratic Regulator Differential Game (LQR-DG) is a robust and optimal control strategy that has been extensively utilized in controlling various nonlinear and complex systems, including quadrotors. This approach employs a linear system model to control its outputs while minimizing a cost function through mini-maximization. The LQR-DG approach has been demonstrated to offer excellent regulation performance and control effort while being robust to external disturbances. For instance, it has been successfully applied to control a ship controller, showcasing its effectiveness and versatility in handling complex control problems [20, 21]. By means of an analytical pursuit-evasion process, the LQR-DG control approach generates precise and optimized control commands. This unique feature sets the LQR-DG controller apart from other conventional optimal control techniques and enables one player to track the most appropriate control command while the other creates disturbances.

This study proposes a new controller for quadrotors based on the LQG technique with integral action, using differential game theory to optimize control performance in the presence of disturbance. Attitude control in the presence of disturbance is essential for ensuring safe and effective quadrotor flight. In order to devise this control approach, a continuous state-space model for a quadrotor's experimental setup is formulated by linearizing the system's equations of motion, which are inherently nonlinear, and identifying its parameters based on experimental data. This approach involves transforming the nonlinear dynamics into a linear system that can be analyzed more readily. The proposed Linear Quadratic Regulator Differential Game (LQR-DG) controller offers an optimal control strategy for generating efficient control commands for quadrotors. The approach employs a two-player system, wherein one player optimizes the command while the other creates disturbances through mini-maximization of a quadratic criterion. This technique not only ensures efficient control but also offers a robust and versatile approach to handle complex control problems. The proposed approach is evaluated against a linear quadratic regulator controller in level flight. The results show that the LQIG-DG controller effectively dissipates disturbances and outperforms the linear quadratic regulator controller. This study presents an important contribution to the development of robust and effective attitude control systems for quadrotors.

The following sections of this research paper provide a comprehensive analysis of the proposed control approach. Section 2 defines the problem, while sections 3 and **??** offer detailed derivations of the dynamics model and the estimation problem for the quadrotor's experimental platform, respectively. Section 4 explicates the proposed LQIG-DG controller architecture. The effectiveness of the controller is evaluated in section 5, which is followed by the conclusion in section 6.

2. Problem Statement

A complex nonlinear system describes the experimental platform of the quadrotor depicted in Figure 1. During its rotation, the quadrotor can adjust its pitch, roll, and yaw angles. An Inertial Measurement Unit (IMU) is used to measure the acceleration and angular velocities along the three orthogonal axes, which are affected by noise. To estimate the states of the quadrotor, including its angular velocities and Euler angles, a nonlinear filter is utilized. A graphical representation of the LQIG-DG controller structure is depicted in Figure 2. The estimated states allow for the stabilization of the quadrotor setup.

Figure 1: 3DoF setup of the quadrotor.

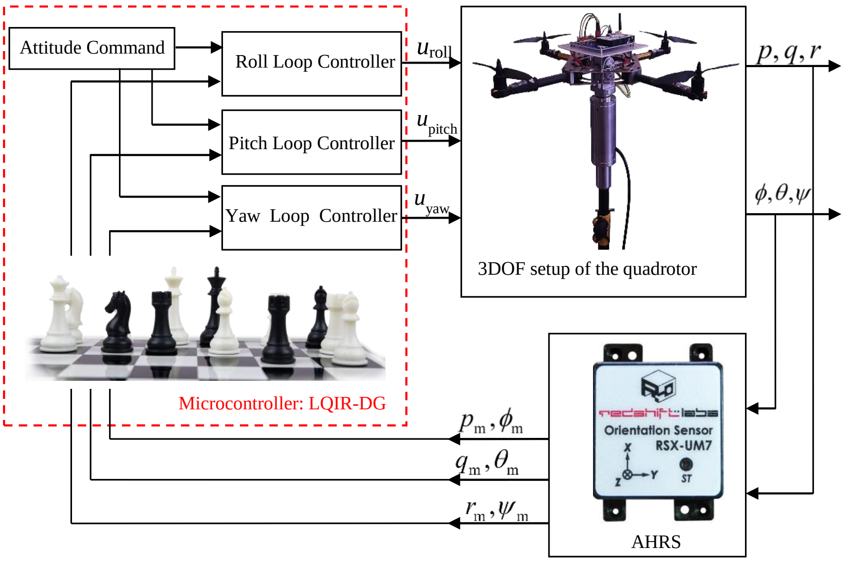

Figure 2: Structure of the LQIG-DG Controller Illustrated in a Block Diagram.

3. Nonlinear Dynamic Model for the Quadrotor Platform

This research paper presents an analysis of the three degrees of freedom for the quadrotor. Furthermore, a state-space model is developed to represent the nonlinear attitude dynamics. A linearization technique is subsequently applied to the model, enabling it to be used as a LQIR-DG control model.

3.1. Quadrotor Configuration and Attitude Dynamics Model

Figure 3 illustrates the quadrotor schematic, depicting four rotors with angular velocity Ω_r rotating around the z_B axis in the body coordinate system. The rotational direction of Rotor 1 and Rotor 3 in the counterclockwise direction counteracts the yawing moment, whereas the clockwise rotation of Rotors 2 and 4 counteracts the yawing moment.

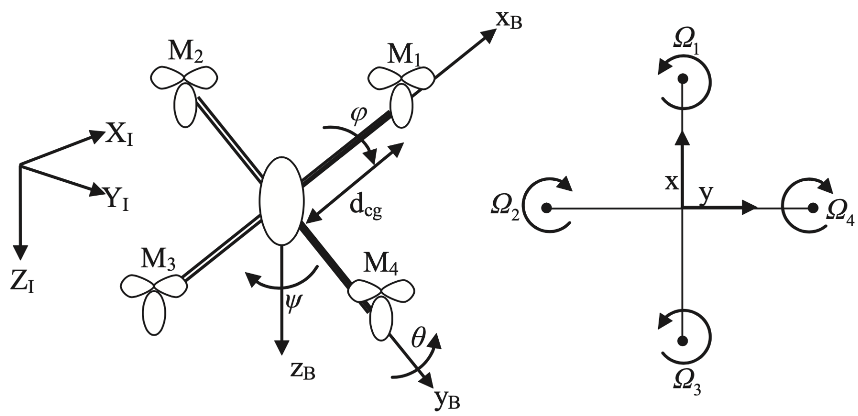

Figure 3: Configuration of the quadrotor.

3.2. Dynamic Modeling of the Quadrotor Platrorm

The dynamic model of the Quadrotor Platrorm is an essential component for control design. In this section, the quadrotor dynamic model is derived using the Newton-Euler method [22, 23].

$$\dot{p} = \frac{\mathrm{I_{yy}} - \mathrm{I_{zz}}}{\mathrm{I_{xx}}} qr + q\frac{\mathrm{I_{rotor}}}{\mathrm{I_{xx}}}\Omega_r + \frac{u_{\mathrm{roll}}}{\mathrm{I_{xx}}} + \frac{d_{\mathrm{roll}}}{\mathrm{I_{xx}}} \tag{1}$$

$$\dot{q} = \frac{\mathrm{I_{zz}} - \mathrm{I_{xx}}}{\mathrm{I_{yy}}} rp + p\frac{\mathrm{I_{rotor}}}{\mathrm{I_{xx}}}\Omega_r + \frac{u_{\mathrm{pitch}}}{\mathrm{I_{yy}}} + \frac{d_{\mathrm{pitch}}}{\mathrm{I_{yy}}} \tag{2}$$

$$\dot{r} = \frac{\mathrm{I_{xx}} - \mathrm{I_{yy}}}{\mathrm{I_{zz}}} pq + \frac{u_{\mathrm{yaw}}}{\mathrm{I_{zz}}} + \frac{d_{\mathrm{yaw}}}{\mathrm{I_{zz}}} \tag{3}$$

The variables (p, q, r) represent the rotational velocities, while the variables d_{roll}, d_{pitch}, and d_{yaw} denote the disturbances produced in x_B, y_B, and z_B, respectively. Additionally, Ixx, Iyy, and Izz are the principal moments of inertia, and Irotor is the rotor inertia about its axis. Euler angle rates are also determined from angular body rates:

$$\begin{bmatrix} \dot{\phi} \\ \dot{\theta} \\ \dot{\psi} \end{bmatrix} \begin{bmatrix} 1 & \sin(\phi)\tan(\theta) & \cos(\phi)\tan(\theta) \\ 0 & \cos(\phi) & -\sin(\phi) \\ 0 & \sin(\phi)/\cos(\theta) & \cos(\phi)/\cos(\theta) \end{bmatrix} \begin{bmatrix} p \\ q \\ r \end{bmatrix} \tag{4}$$

The quadrotor system has three degrees of freedom: roll, pitch, and yaw. The rotational motion is described by the angles (ϕ, θ, ψ), which represent roll, pitch, and yaw, respectively. The residual rotor velocity, denoted by ω_r, is calculated as follows:

$$\Omega_r = -\Omega_1 + \Omega_2 - \Omega_3 + \Omega_4 \tag{5}$$

3.3. Innovative Control Strategies for Quadrotor

The control inputs u_{roll}, u_{pitch}, and u_{yaw} correspond to the moments generated by the quadrotor's rotors along the roll, pitch, and yaw axes, respectively, and are defined as follows:

$$u_{\text{roll}} = \mathrm{b}\,\mathrm{d_{cg}}(\Omega_2^2 - \Omega_4^2) \tag{6}$$

$$u_{\text{pitch}} = \mathrm{b}\,\mathrm{d_{cg}}(\Omega_1^2 - \Omega_3^2) \tag{7}$$

$$u_{\text{yaw}} = \mathrm{d}(\Omega_1^2 - \Omega_2^2 + \Omega_3^2 - \Omega_4^2) \tag{8}$$

The quadrotor's drag and thrust coefficients are denoted by d and b, respectively. The distance between the rotors and the gravity center is represented by $\mathrm{d_{cg}}$. The angular velocity commands can be computed as follows:

$$\Omega_{c,1}^2 = \Omega_{\text{mean}}^2 + \frac{1}{2\mathrm{b}\,\mathrm{d_{cg}}} u_{\text{pitch}} + \frac{1}{4d} u_{\text{yaw}} \tag{9}$$

$$\Omega_{c,2}^2 = \Omega_{\text{mean}}^2 + \frac{1}{2\mathrm{b}\,\mathrm{d_{cg}}} u_{\text{roll}} - \frac{1}{4d} u_{\text{yaw}} \tag{10}$$

$$\Omega_{c,3}^2 = \Omega_{\text{mean}}^2 - \frac{1}{2\mathrm{b}\,\mathrm{d_{cg}}} u_{\text{pitch}} + \frac{1}{4d} u_{\text{yaw}} \tag{11}$$

$$\Omega_{c,4}^2 = \Omega_{\text{mean}}^2 - \frac{1}{2\mathrm{b}\,\mathrm{d_{cg}}} u_{\text{roll}} - \frac{1}{4d} u_{\text{yaw}} \tag{12}$$

The nominal angular velocities of the rotors are denoted by Ω_{mean}.

3.4. State-Space Representation of Quadrotor Dynamics

The formulation of a state-space model is crucial for the development of advanced control strategies. In this context, a state-space representation of the quadrotor system is provided in order to facilitate the design of control algorithms.

In order for the quadrotor to be controlled, it can be modelled in state-space by introducing the following variables: $x_1 = p$, $x_2 = q$, $x_3 = r$, $x_4 = \phi$, $x_5 = \theta$, and $x_6 = \psi$.

$$\dot{x}_1 = \Gamma_1 x_2 x_3 + \Gamma_2 x_2 \Omega_r + \Gamma_3 u_{\text{roll}} + \Gamma_3 d_{\text{roll}} \tag{13}$$

$$\dot{x}_2 = \Gamma_4 x_1 x_3 - \Gamma_5 x_1 \Omega_r + \Gamma_6 u_{\text{pitch}} + \Gamma_6 d_{\text{pitch}} \tag{14}$$

$$\dot{x}_3 = \Gamma_7 x_1 x_2 + \Gamma_8 u_{\text{yaw}} + \Gamma_8 d_{\text{yaw}} \tag{15}$$

$$\dot{x}_4 = x_1 + (x_2 \sin(x_4) + x_3 \cos(x_4)) \tan(x_5) \tag{16}$$

$$\dot{x}_5 = x_2 \cos(x_4) - x_3 \sin(x_4) \tag{17}$$

$$\dot{x}_6 = (x_2 \sin(x_4) + x_3 \cos(x_4)) / \cos(x_5) \tag{18}$$

Furthermore, to facilitate the analysis, $\Gamma_i (i = 1, \ldots, 8)$ is introduced, which represents a set of coefficients related to the quadrotor's physical properties and external factors.

$$\begin{aligned}
\Gamma_1 &= \frac{\mathrm{I_{yy}} - \mathrm{I_{zz}}}{\mathrm{I_{xx}}}, \quad \Gamma_2 = \frac{\mathrm{I_{rotor}}}{\mathrm{I_{xx}}}, \quad \Gamma_3 = \frac{1}{\mathrm{I_{xx}}} \\
\Gamma_4 &= \frac{\mathrm{I_{zz}} - \mathrm{I_{xx}}}{\mathrm{I_{yy}}}, \quad \Gamma_5 = \frac{\mathrm{I_{rotor}}}{\mathrm{I_{xx}}}, \quad \Gamma_6 = \frac{1}{\mathrm{I_{yy}}} \\
\Gamma_7 &= \frac{\mathrm{I_{xx}} - \mathrm{I_{yy}}}{\mathrm{I_{zz}}}, \quad \Gamma_8 = \frac{1}{\mathrm{I_{zz}}}
\end{aligned} \tag{19}$$

The attitude states and gyro measurements are represented as vectors, denoted by **z** and **m**, respectively. The attitude state vector is defined as follows:

$$\mathbf{z} = \begin{bmatrix} p_m \; q_m \; r_m \; \phi_m \; \theta_m \; \psi_m \end{bmatrix} \tag{20}$$

Note that the vector is transposed using the superscript T to indicate that it is a row vector.

3.5. Linearization of the Nonlinear Quadrotor Model

The application of a continuous-time linear model facilitates the efficient control of the quadrotor. The linear state-space model can be represented as follows:

$$\dot{\mathbf{x}}(t) = \mathbf{A}\,\mathbf{x}(t) + \mathbf{B}\,\mathbf{u}(t) + \mathbf{B_d}\,\mathbf{d}(t) \tag{21}$$

The system's input and disturbance matrices, denoted as $\mathbf{B}$ and $\mathbf{B_d}$ respectively, with $\mathbf{d}$ representing the disturbance, are part of the system's dynamics, represented by the matrix $\mathbf{A}$. The measurement equation is given by

$$\mathbf{z}(t) = \mathbf{x}(t) \tag{22}$$

The differential equations presented in Equations (13)-(18) allow for the development of a corresponding linear dynamic model for the quadrotor platform at its equilibrium points ($\mathbf{x}_e! =!0$ and $\mathbf{u}_e! =!0$). This model can be expressed as follows:

$$\begin{aligned}\dot{\mathbf{x}} = \begin{bmatrix} \dot{\mathbf{x}}_{\text{roll}} \\ \dot{\mathbf{x}}_{\text{pitch}} \\ \dot{\mathbf{x}}_{\text{yaw}} \end{bmatrix} &= \begin{bmatrix} \mathbf{A}_{\text{roll}} & \mathbf{0} & \mathbf{0} \\ \mathbf{0} & \mathbf{A}_{\text{pitch}} & \mathbf{0} \\ \mathbf{0} & \mathbf{0} & \mathbf{A}_{\text{yaw}} \end{bmatrix} \begin{bmatrix} \mathbf{x}_{\text{roll}} \\ \mathbf{x}_{\text{pitch}} \\ \mathbf{x}_{\text{yaw}} \end{bmatrix} \\ &+ \begin{bmatrix} \mathbf{B}_{\text{roll}} & \mathbf{0} & \mathbf{0} \\ \mathbf{0} & \mathbf{B}_{\text{pitch}} & \mathbf{0} \\ \mathbf{0} & \mathbf{0} & \mathbf{B}_{\text{yaw}} \end{bmatrix} \begin{bmatrix} \mathbf{u}_{\text{roll}} \\ \mathbf{u}_{\text{pitch}} \\ \mathbf{u}_{\text{yaw}} \end{bmatrix} \\ &+ \begin{bmatrix} \mathbf{B}_{\text{roll}} & \mathbf{0} & \mathbf{0} \\ \mathbf{0} & \mathbf{B}_{\text{pitch}} & \mathbf{0} \\ \mathbf{0} & \mathbf{0} & \mathbf{B}_{\text{yaw}} \end{bmatrix} \begin{bmatrix} \mathbf{d}_{\text{roll}} \\ \mathbf{d}_{\text{pitch}} \\ \mathbf{d}_{\text{yaw}} \end{bmatrix}\end{aligned} \tag{23}$$

where $\mathbf{x}_{\text{roll}} = \begin{bmatrix} p & \phi \end{bmatrix}^{\text{T}}$, $\mathbf{x}_{\text{pitch}} = \begin{bmatrix} q & \theta \end{bmatrix}^{\text{T}}$, and $\mathbf{x}_{\text{yaw}} = \begin{bmatrix} r & \psi \end{bmatrix}^{\text{T}}$.

In addition, the input matrices and state are shown as

$$\mathbf{A}_{\text{roll}} = \mathbf{A}_{\text{pitch}} = \mathbf{A}_{\text{yaw}} = \begin{bmatrix} 0 & 0 \\ 1 & 0 \end{bmatrix} \tag{24}$$

$$\mathbf{B}_{\text{roll}} = \begin{bmatrix} \frac{1}{\text{I}_{\text{xx}}} \\ 0 \end{bmatrix};\; \mathbf{B}_{\text{pitch}} = \begin{bmatrix} \frac{1}{\text{I}_{\text{yy}}} \\ 0 \end{bmatrix};\; \mathbf{B}_{\text{yaw}} = \begin{bmatrix} \frac{1}{\text{I}_{\text{zz}}} \\ 0 \end{bmatrix} \tag{25}$$

3.6. Identification of the Setup Parameters

This section presents an optimization technique for estimating the model parameters (Γ) of the 3DOF experimental setup from experimental data. The technique is based on the Nonlinear Least Squares (NLS) method, which is widely used in parameter estimation problems. The NLS algorithm utilizes the trust-region reflective least squares (TRRLS) method to iteratively find the values of the model parameters. The goal is to minimize a cost function, which is based on the sum of squares between the input/output signals provided by the simulation model and the experimental ones.

The optimization process involves finding a vector $\mathbf{\Gamma}$ that minimizes the cost function. This is achieved by iteratively updating the values of the model parameters until convergence is achieved. The NLS method is particularly useful for problems where the model is nonlinear and the measurement noise is known. The approach is based on a least squares problem, where the objective is to find the values of $\mathbf{\Gamma}$ that minimize the sum of squares function [24]:

$$\min_{\Gamma_i}\left(\| e(\Gamma_i) \|^2\right) = \min_{\Gamma_i} = \left(\sum_{i=1}^{n}(y-\hat{y})^2\right) \tag{26}$$

where y and $\hat{y}$ are the experimental and simulated output signals, when the same input signals are applied ones. The structure of the proposed identification approach is illustrated in Figure 4.

In summary, the NLS optimization technique is an effective approach for estimating the model parameters of the 3DOF experimental setup from experimental data. The technique utilizes the TRRLS method to iteratively update the values of the model parameters, with the goal of minimizing the difference between the simulation model and the experimental data.

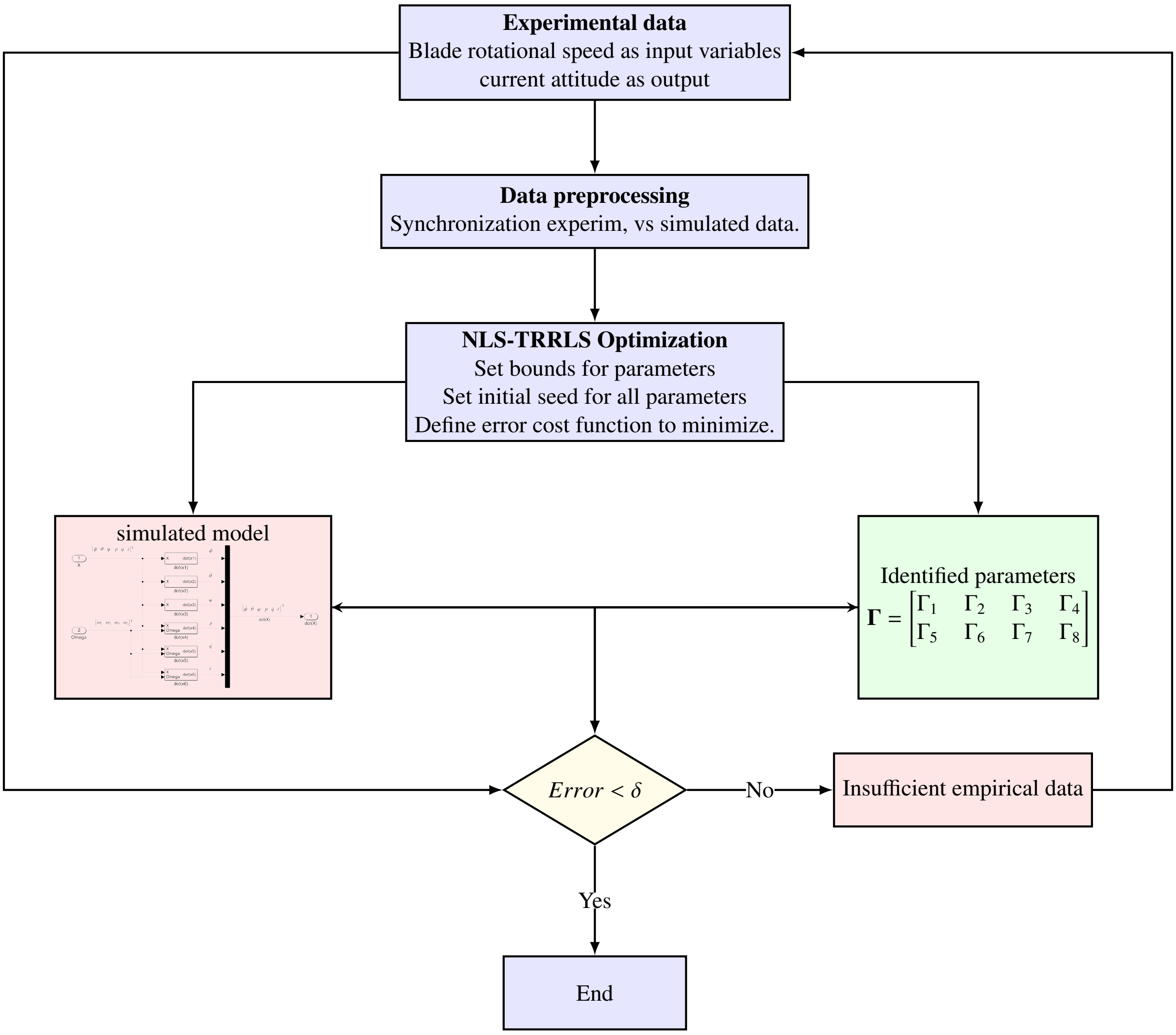

Figure 4: Structure of TRRLS identification approach.

4. Optimal Control Strategy Formulation for a Nonlinear System

The LQR-DG controller is augmented with an integral action to eliminate steady-state errors in desired following. The first step in the controller design is to define the augmented state space of the linear quadrotor model to incorporate it into the controller architecture. Subsequently, the LQR-DG controller design procedure is introduced to generate optimal control commands for the experimental quadrotor setup.

4.1. Augmented State Space Formulation

To add the integral action to the controller structure, the augmented states are defined as follows:

$$\mathbf{x_{a_i}} = \begin{bmatrix} \mathbf{x_i} & \int \mathbf{x_i} \end{bmatrix}^{\mathrm{T}} \tag{27}$$

The quadrotor dynamics model, as represented by Eq. (21), is transformed into an augmented state-space model that incorporates the roll (ϕ), pitch (θ), and yaw (ψ) angles. The augmented state-space model provides a comprehensive description of the quadrotor's dynamic behavior, enabling the design of effective control strategies. The resulting augmented state-space model is expressed as follows:

$$\dot{\mathbf{x}}_{\boldsymbol{a}}(t) = \mathbf{A_a}\mathbf{x_a}(t) + \mathbf{B_a}\mathbf{u}(t) + \mathbf{B_{d_a}}\mathbf{d}(t) \tag{28}$$

where matrices $\mathbf{A_a}$ and $\mathbf{B_a}$ are Presented as:

$$\mathbf{A_a} = \begin{bmatrix} \mathbf{A} & \mathbf{0} \\ \mathbf{I} & \mathbf{0} \end{bmatrix} \tag{29}$$

$$\mathbf{B_a} = \mathbf{B_{d_a}} = \begin{bmatrix} \mathbf{B} \\ \mathbf{0} \end{bmatrix} \tag{30}$$

In the preceding equation, the symbol $\mathbf{I}$ represents the identity matrix.

4.2. LQIR-DG Control Scheme with Integral Action for Quadrotor

Based on differential game theory, the LQIR-DG controller is a robust and optimal method. This controller is comprised of two key players, where one is responsible for finding the best control command, while the other aims to create the worst disturbance. The primary objective of the first player is to minimize a cost function, whereas the second player attempts to maximize it. Accordingly, the quadratic cost function equation can be represented using min-max operators in the following manner:

$$\min_{u}\max_{d} J(\mathbf{x_{a_i}}, u_i, d_i) = J(\mathbf{x_{a_i}}, u_i^*, d_i^*) = \min_{u}\max_{d} \int_0^{\mathrm{t_f}} \left(\mathbf{x_{a_i}^T}\mathbf{Q_i}\mathbf{x_{a_i}} + u_i^{\mathrm{T}} R u_i - d_i^{\mathrm{T}} R_d d_i\right) \mathrm{d}t \tag{31}$$

The matrices R and R_d in the aforementioned equation are symmetric nonnegative definite matrices, while $\mathbf{Q_i}$ is a symmetric positive definite matrix. The final time is denoted by $\mathrm{t_f}$. To tackle this problem, the relationship between the general optimal problem and the LQIR problem is established [25]. As a result, the optimal control input for each control loop can be obtained as follows:

$$u_i(t) = -\mathbf{K}_{\boldsymbol{i}}(t)\mathbf{x_{a_i}}(t) \tag{32}$$

$$d_i(t) = \mathbf{K_{d_i}}(t)\mathbf{x_{a_i}}(t) \tag{33}$$

where $\mathbf{K_i}$ and $\mathbf{K_{d_i}}$ are a time varying gain, defined as follows:

$$\mathbf{K_i} = R^{-1}\mathbf{B}_{\boldsymbol{a_i}}^{\mathbf{T}}\mathbf{P}_{\boldsymbol{a_i}}(t) \tag{34}$$

$$\mathbf{K_{d_i}} = R_d^{-1}\mathbf{B}_{\boldsymbol{a_{d_i}}}^{\mathbf{T}}\mathbf{P}_{\boldsymbol{a_{d_i}}}(t) \tag{35}$$

where $\mathbf{P}_{a_i}(t)$ and $\mathbf{P}_{a_{d_i}}(t)$ satisfy

$$\dot{\mathbf{P}}_{a_i}(t) = -\mathbf{A}_{\mathbf{a}}^{\mathbf{T}}\mathbf{P}_{\mathbf{a_i}}(t) - \mathbf{P}_{\mathbf{a_i}}(t)\mathbf{A}_{\mathbf{a}} - \mathbf{Q}_{\mathbf{i}} + \mathbf{P}_{\mathbf{a_i}}(t)\mathbf{S}_{\mathbf{a_i}}(t)\mathbf{P}_{\mathbf{a_i}}(t) + \mathbf{P}_{\mathbf{a_i}}(t)\mathbf{S}_{\mathbf{a_{d_i}}}(t)\mathbf{P}_{\mathbf{a_{d_i}}}(t) \tag{36}$$

$$\dot{\mathbf{P}}_{a_{d_i}}(t) = -\mathbf{A}_{\mathbf{a}}^{\mathbf{T}}\mathbf{P}_{\mathbf{a_{d_i}}}(t) - \mathbf{P}_{\mathbf{a_{d_i}}}(t)\mathbf{A}_{\mathbf{a}} - \mathbf{Q}_{\mathbf{i}} + \mathbf{P}_{\mathbf{a_{d_i}}}(t)\mathbf{S}_{\mathbf{a_{d_i}}}(t)\mathbf{P}_{\mathbf{a_{d_i}}}(t) + \mathbf{P}_{\mathbf{a_{d_i}}}(t)\mathbf{S}_{\mathbf{a_i}}(t)\mathbf{P}_{\mathbf{a_i}}(t) \tag{37}$$

where $\mathbf{S}_{\mathbf{a_i}} = \mathbf{B}_{\mathbf{a_i}}R^{-1}\mathbf{B}_{a_i}^{\mathbf{T}}$ and $\mathbf{S}_{\mathbf{a_{d_i}}} = \mathbf{B}_{a_{d_i}}R_d^{-1}\mathbf{B}_{a_{d_i}}^{\mathbf{T}}$. In the present study, the feedback control law is generated using the steady-state values of the aforementioned equations as t_f tends to infinity.

5. Experimental Findings and Analysis

Here, the study presents the results of applying the LQIR-DG controller method to the control loops of roll, pitch, and yaw of an experimental quadrotor setup. To ensure optimal and robust performance, the controller parameters are tuned using the results of numerical simulations. Additionally, the study compares the performance of the LQIR-DG controller to that of other controllers, including LQR, PID, and LQIR control strategies. The quadrotor's parameters are detailed in Table 1.

Moreover, the parameters of LQIR-DG controller weight are denoted in table 2.

Table 1: The Parameter of the Quadrotor

Parameter	***Value***	***Unit***
I_{xx}	0.02839	kg.m^2
I_{yy}	0.03066	kg.m^2
I_{zz}	0.0439	kg.m^2
I_{rotor}	4.4398×10^{-5}	kg.m^2
b	3.13×10^{-5}	N. sec^2 /rad^2
d	3.2×10^{-6}	N.m. sec^2 /rad^2
Ω_{mean}	3000	rpm
d_{cg}	0.2	m

Table 2: The Parameters of the LQIR-DG Controller

Control Loop	***Weight***	***Value***
Roll	$\mathbf{Q}_{roll}$	diag([0.02, 65.96, 83.04, 0.00])
Pitch	$\mathbf{Q}_{pitch}$	diag([435.01, 262.60, 262.60, 0.00])
Yaw	$\mathbf{Q}_{yaw}$	diag([$4e{-}4$, 0.00, 0.133, 0])
-	R	1
-	R_d	1.2764

5.1. Identification of the 3DoF experimental setup model

As denoted in section 3.4, the parameters of the quadrotor setup are $\Gamma_i (i = 1, ..., 8)$ that need to be identified based on the NRS algorithm. The NLS-TRRLS algorithm is performed in the Matlab R2022b®. In order to increase accuracy identification of parameters, three scenarios, according to Error! Reference source not found., are considered and performed. When the stopping condition of the NLS algorithm is reached, the best values of the quadrotor parameters are computed, shown in Table 4. Moreover, the intelligent movement of the parameters during the optimization process for finding the true values is shown in Figure 4. In the first scenario, according to the Figure 5, the quadrotor is able to rotate about only one axis (roll, pitch or yaw axes) to identify Γ_3 , Γ_6 and Γ_8 parameters. In the second scenario, Figure 6 shows Γ_2 and Γ_5 parameters are estimated based on the experimental setup, that is free to rotate around its roll and pitch axes. Finally, in the last scenario, according to the Figure 7, Γ_1 , Γ_4 and Γ_7 parameters of the UAV model are identified by rotate the quadrotor setup around three axis. These results illustrate that the outputs of the simulation results for the quadrotor model are consistent with reality.

Table 3: Scenarios for identification of quadrotor model.

Scenario	***Description***	***Initial Conditions***	***angular velocity Commands***
I	Roll free	38	2000 2000 2000 3400
	Pitch free	-15	3700 2000 2000 2000
	Yaw free	-75	2000 3300 2000 3300
II	Roll and Pitch free	$8 \quad -5$	1700 3800 2400 1700
III	Roll, Pitch, and Yaw free	$8 \quad -3 \quad -146$	1700 3800 2400 1700

Table 4: True values of the quadrotor parameters.

Parameter	***Value***	**Parameter**	***Value***
Γ_1	-0.9622	Γ_5	3.6441×10^{-4}
Γ_2	-0.0154	Γ_6	7.5395×10^{-5}
Γ_3	5.4716×10^{-5}	Γ_7	0.1308
Γ_4	1.0457	Γ_8	4.3753×10^{-5}

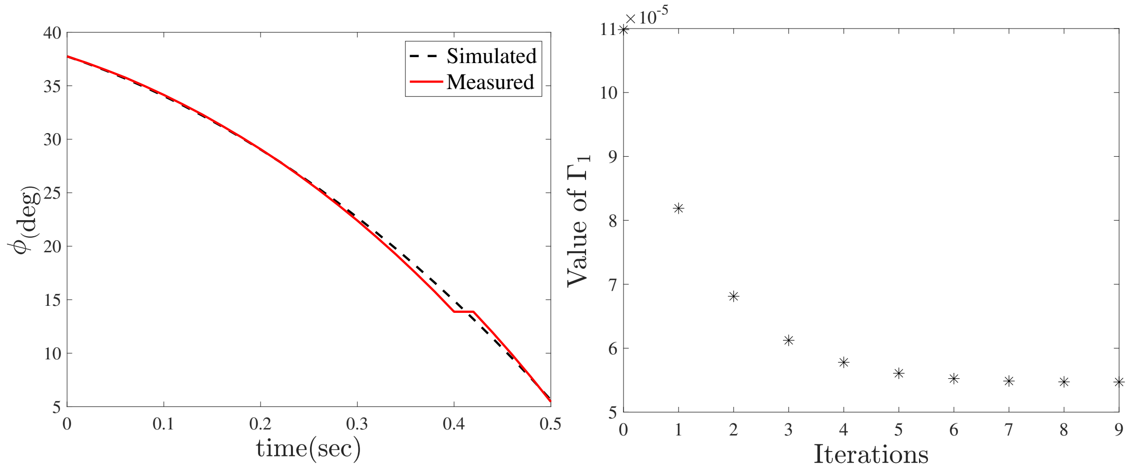

(a)

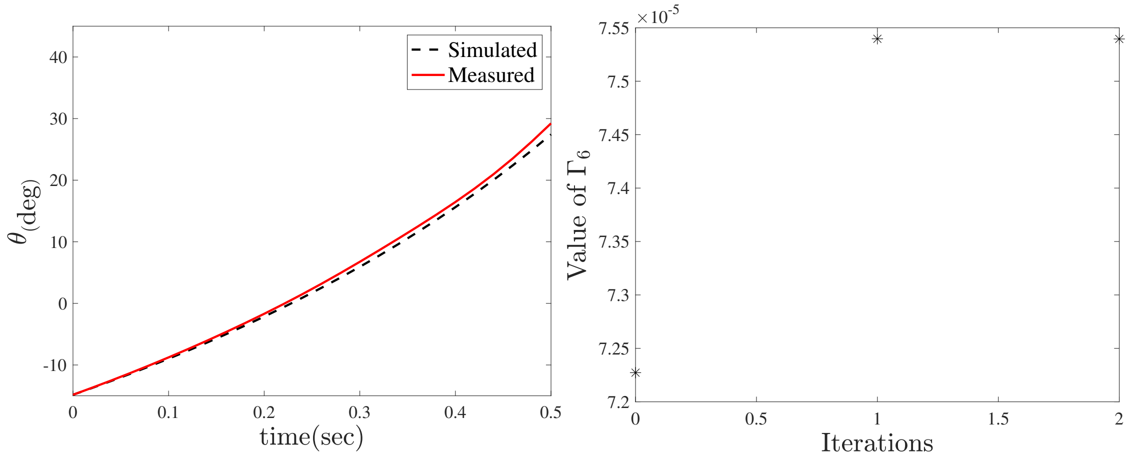

(b)

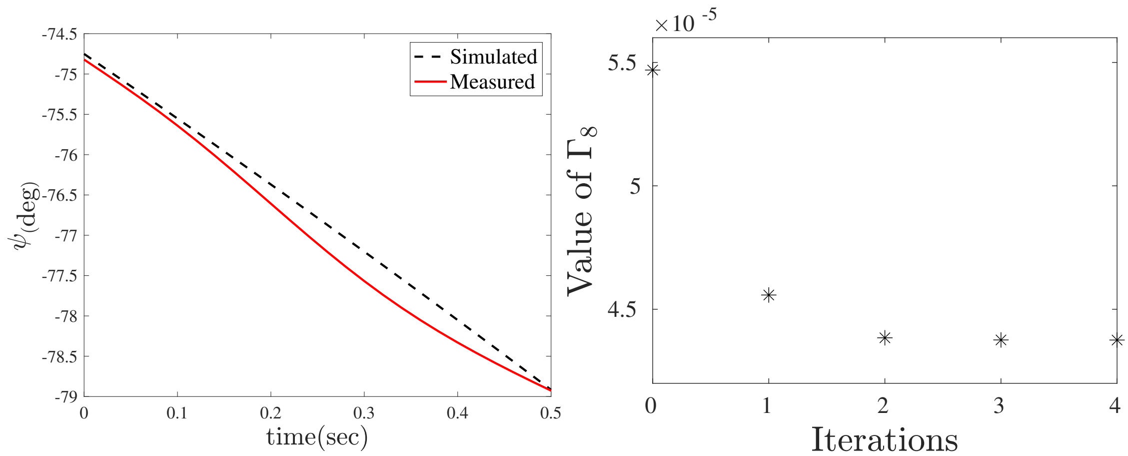

(c)

Figure 5: Identification process results when the quadrotor rotates about only one axis: (a) Identification of Γ_3 in free roll. (b) Identification of Γ_6 in free pitch. (c) Identification of Γ_8 in free yaw.

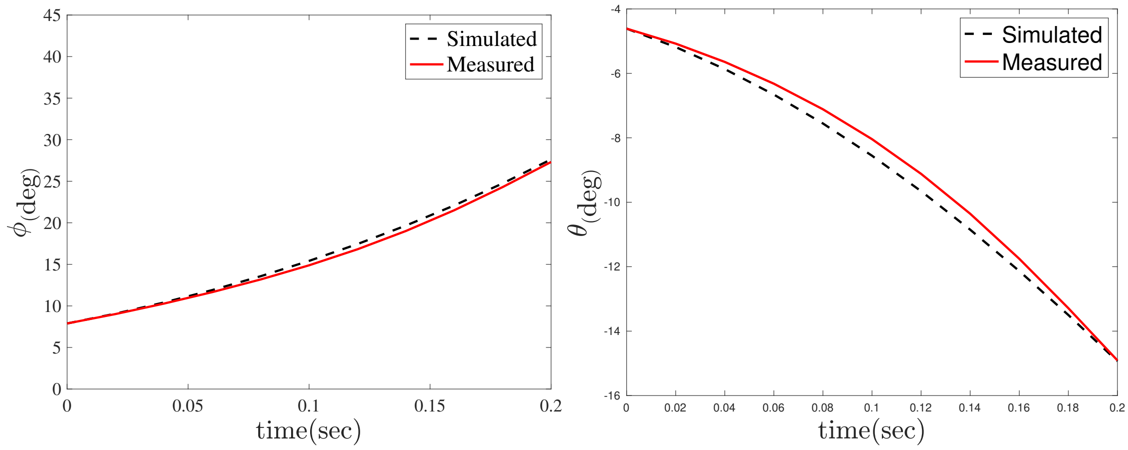

(a)

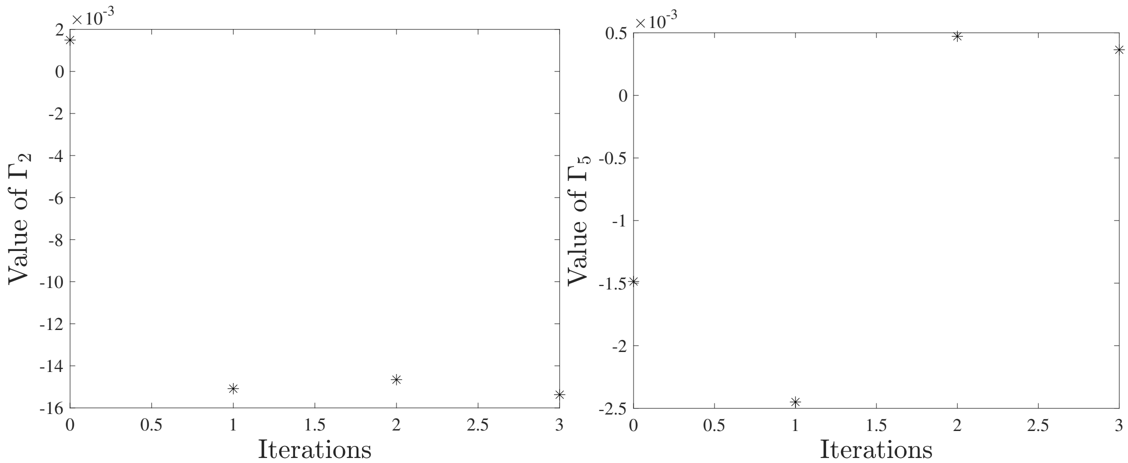

(b)

Figure 6: Identification process results when the quadrotor rotates about its roll and pitch axes: (a) Comparison of Simulation and experimental results. (b) Identification of Γ_2 and Γ_5.

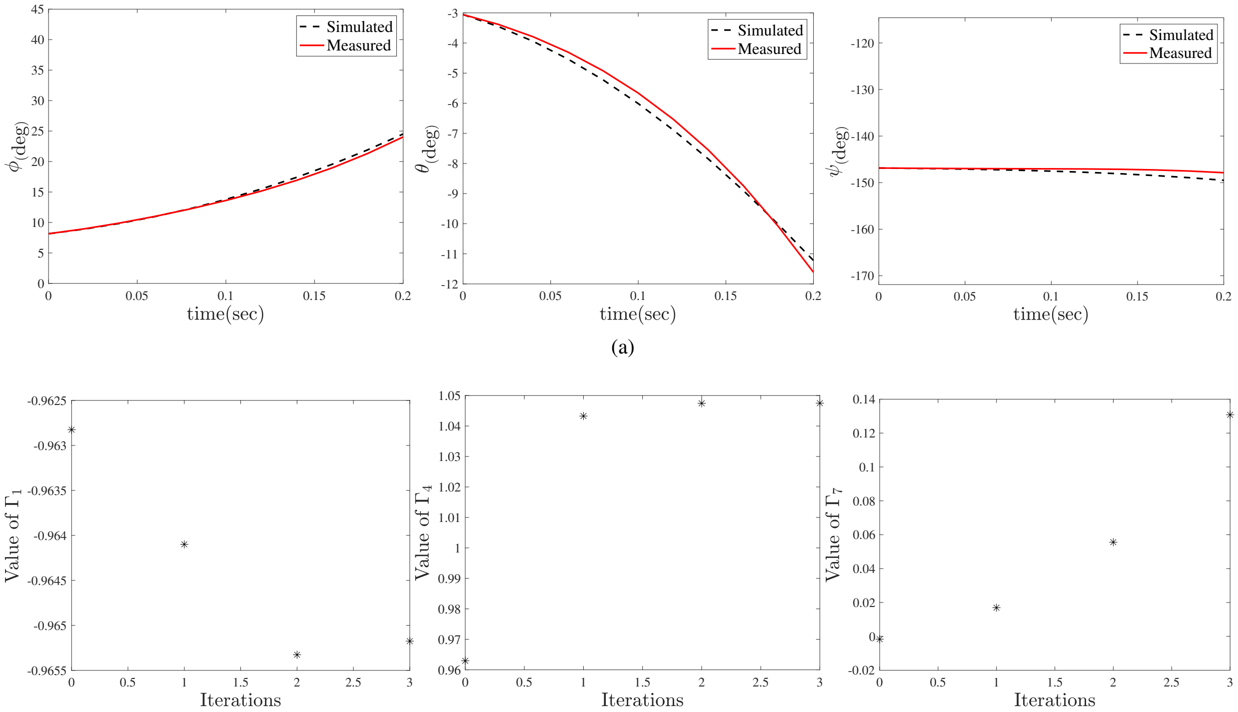

Figure 7: Identification process results when the quadrotor rotates about its roll, pitch, and yaw axes: (a) Comparison of Simulation and experimental results. (b) Identification of Γ_1 , Γ_4 and Γ_7 parameters.

5.2. Assessment of LQIR-DG Control Strategy

The performance of the LQIR-DG control strategy is assessed in three aspects: regulation and following of a square wave reference signal, disturbance rejection, and model uncertainty. The regulation and following of the square wave reference signal are examined in Section 5.2.1. The effectiveness of the controller in rejecting different levels of disturbance is evaluated in Section 5.2.2. Moreover, the impact of model uncertainty on the performance of the controller is studied in Section 5.2.3.

5.2.1. Regulating and Following Square Wave

This experiment evaluates the performance of the LQIR-DG controller in regulating and following a square wave input for the quadrotor's attitude angles. The desired square wave input is generated for the roll, and pitch angles. The experiment's results demonstrate the effectiveness of the LQIR-DG controller in accurately tracking the square wave input

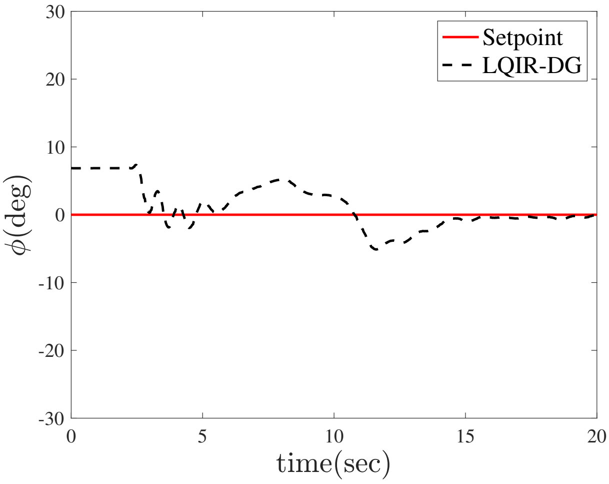

(a)

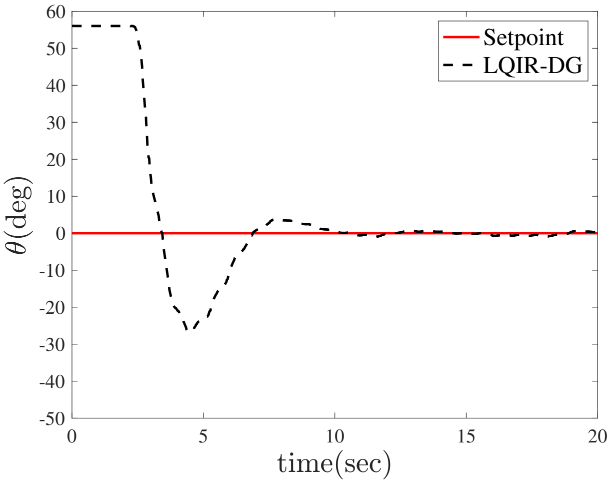

(b)

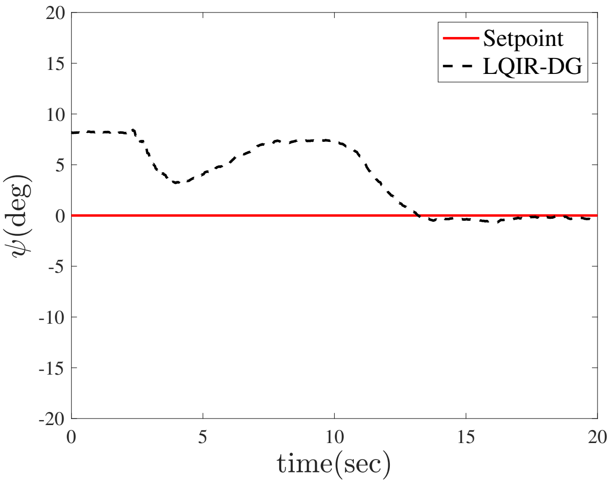

(c)

Figure 8: Performance of the LQIR-DG controller (a) roll angle (b) pitch angle (c) yaw angle

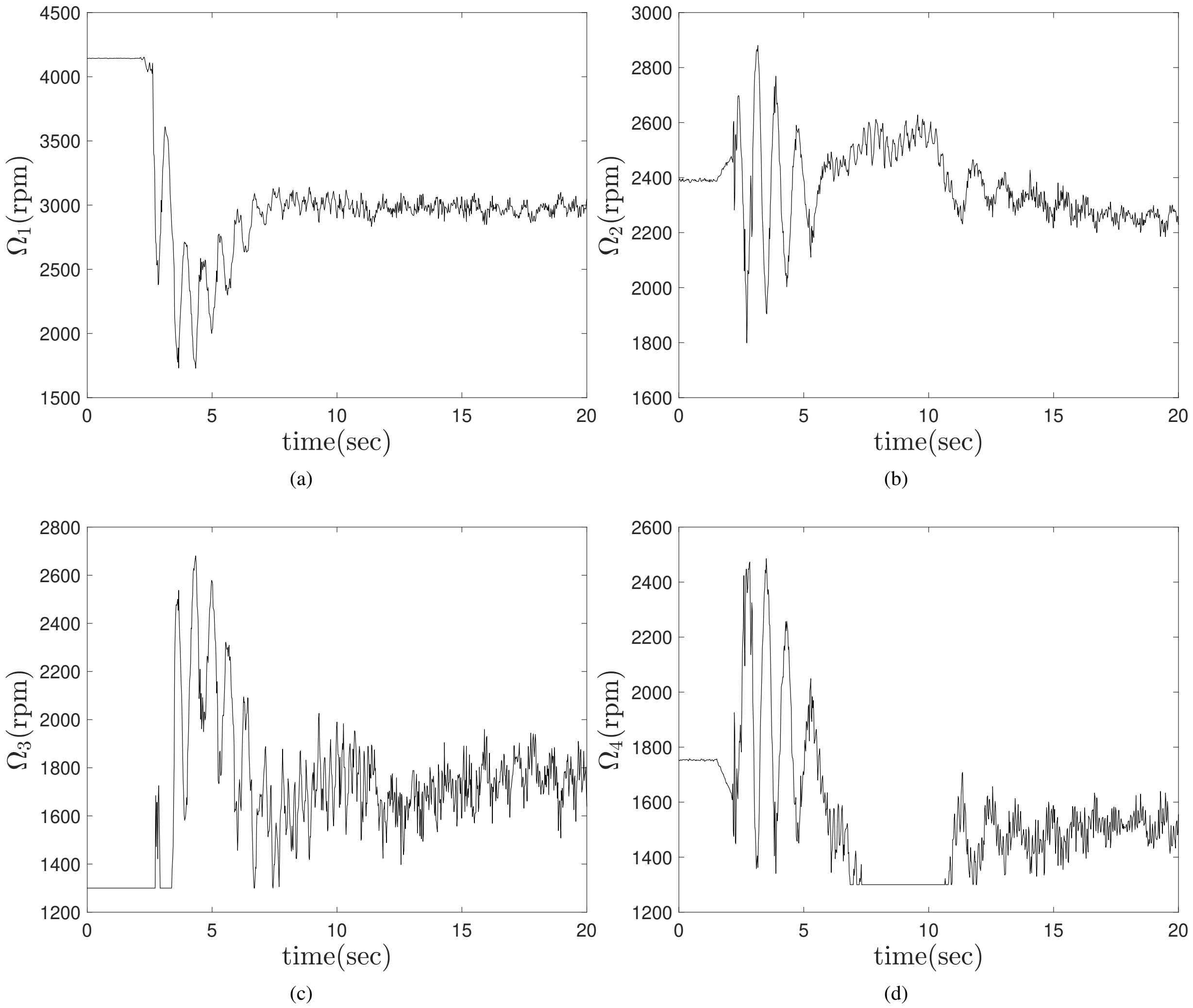

Figure 9: Time history of angular velocity commands

Figure 10 illustrates the performance of the LQIR-DG controller in the coupling mode of the roll and pitch channels to track the desired angle as a square wave with a frequency of 0.02 Hz and an amplitude of 20 degrees.

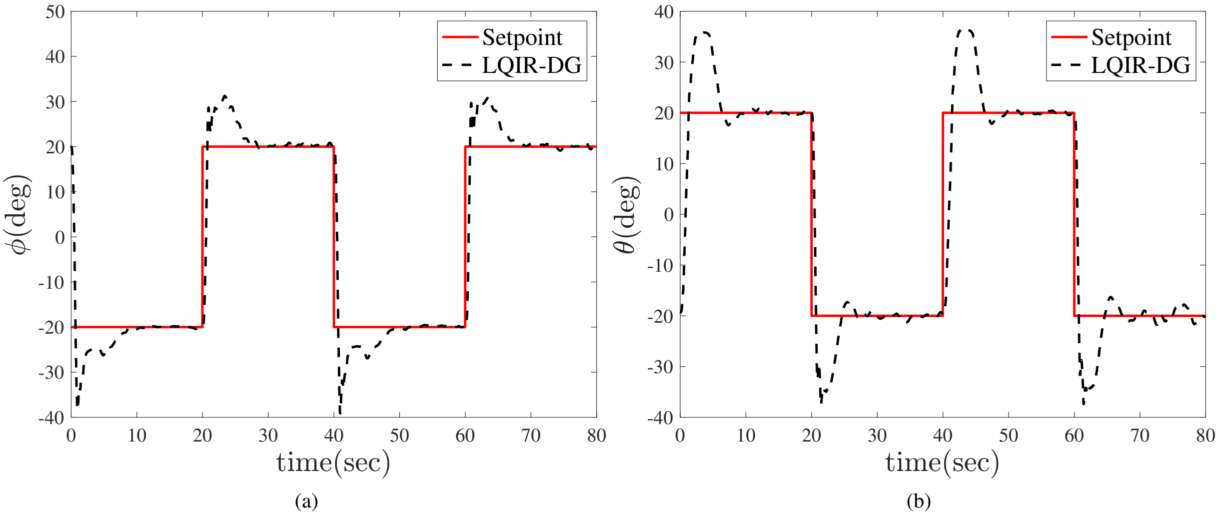

Figure 10: LQIR-DDG controller performance in order to track the desired angles in the two-degree-of-freedom coupling mode (a) Comparison of the roll angle with the desired value (b) Comparison of the pitch angle with the desired

5.2.2. *Investigating the possibility of disturbance rejection*

This section investigates the possible rejection of input disturbances by the LQIR-DG controller in regulation. For this purpose, a disturbance with an amplitude of 0.5 N is added to the input from 20 to 60 seconds. As shown in figure 11, the LQIR-DG controller performs well in coupling the roll and screw channels to remove the input disturbance. 11 (a), the performance of this controller is checked by comparing the desired roll angle with the actual roll angle. Also, 11 (b) compares the desired pitch angle with the actual pitch angle of the 3DoF experimental setup in removing the input disturbance. The results indicate the proper performance of the controller in removing the input disturbance.

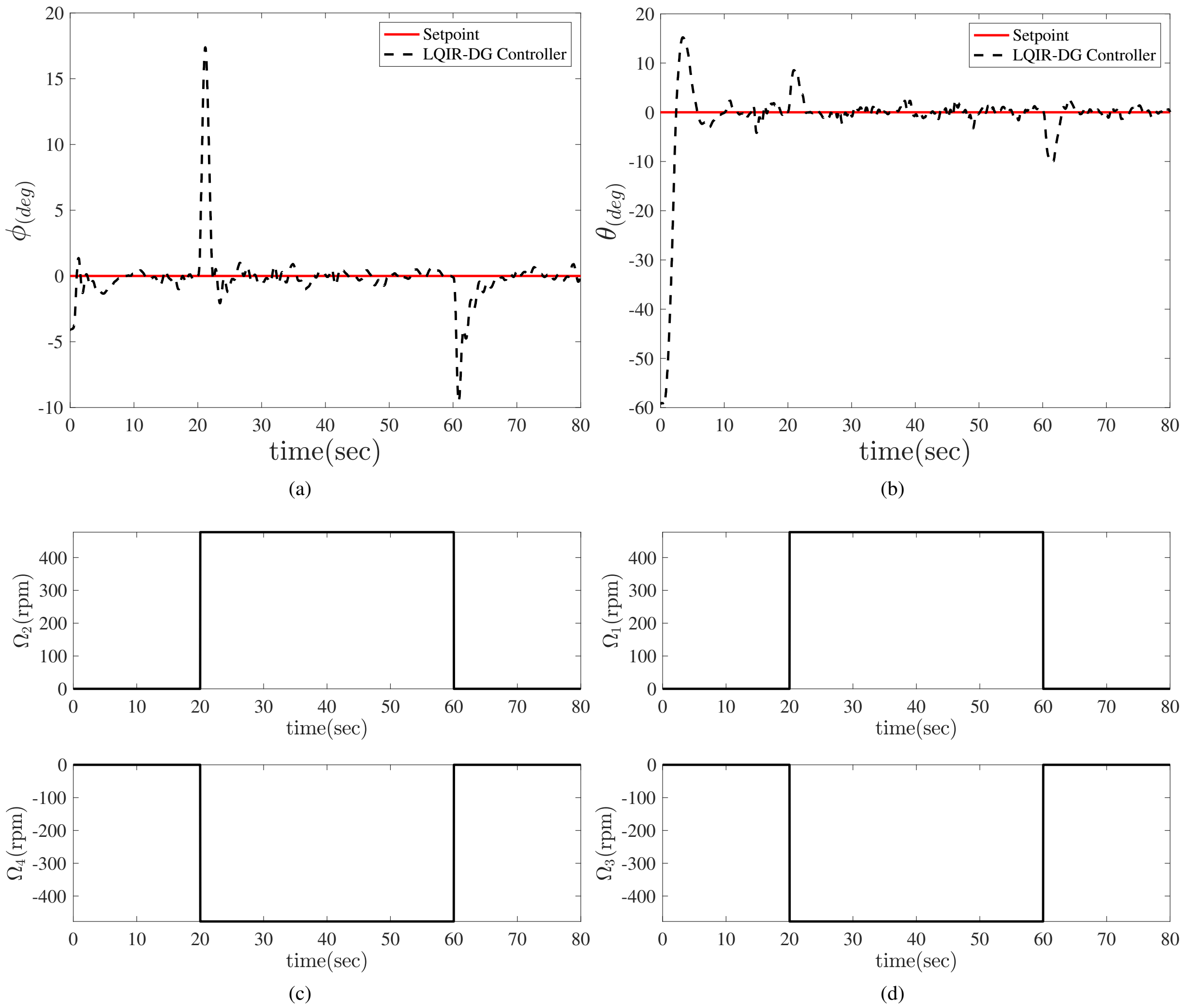

Figure 11: The performance of the LQIR-DG controller in the presence of the input disturbance in the two-degree-of-freedom coupling mode (a) Comparison of the desired roll angle with the actual value (b) Comparison of the desired pitch angle with the actual value.

5.2.3. Investigating the impact of uncertainty in modeling

This section examines the performance of the LQIR-DG controller designed by considering the uncertainty in 3DoF experimental setup modeling. The performance of the sliding mode controller in the coupling mode of the roll, pitch, and yaw channels is checked by considering the uncertainty in the 3DoF experimental setup modeling in figure 13. For this purpose, 50 grams is added to the roll axis and 100 grams to the pitch axis. In figure 13 (a), the performance of this controller is checked by comparing the desired roll angle with the actual roll angle; In figure 13 (b), the performance of this controller is checked by comparing the desired pitch angle to the actual pitch angle. The implementation results indicate the proper efficiency of the LQIR-DG controller in pursuit of the desired value, taking into account the uncertainty in the values of the moments of inertia around each axis of the body coordinate system.

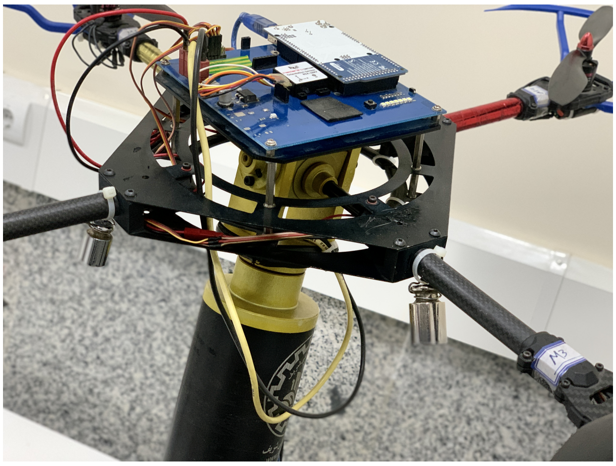

Figure 12: 3DoF setup of the quadrotor with added weight

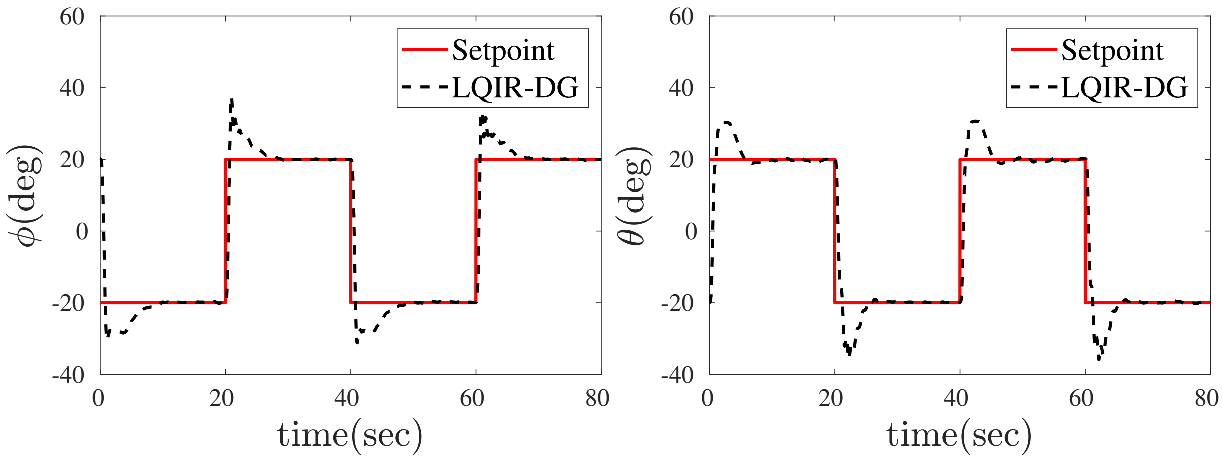

(a)

(b)

Figure 13: The performance of the LQIR-DG controller by adding weight to each of the roll and pitch axes in the two-degree-of-freedom coupling mode (a) Comparison of the roll angle with the actual value (b) Comparison of the pitch angle with the actual value

5.2.4. Comparison with LQR, LQIR, and PID

Here, the LQIR-DG controller performance is compared with famous control strategies such as the LQR controller method. Figure14 compares the quadrotor's desired and actual pitch angle in the presence of these controllers. This result indicates that the LQIR-DG controller can provide high tracking performance, such as good transient response and high rapid convergence relative to the LQR controller for pitch angle control of the quadrotor setup.

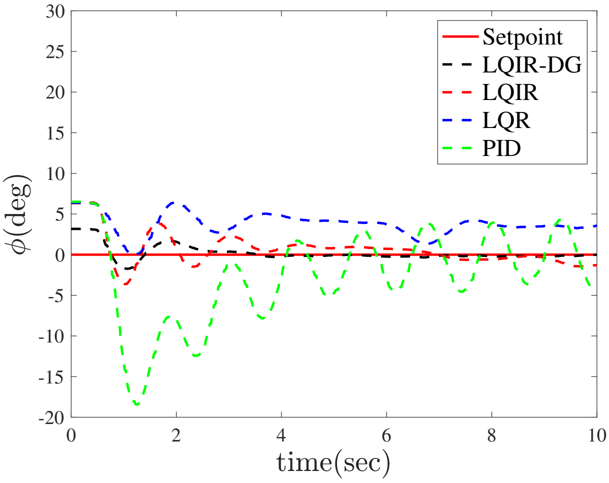

(a)

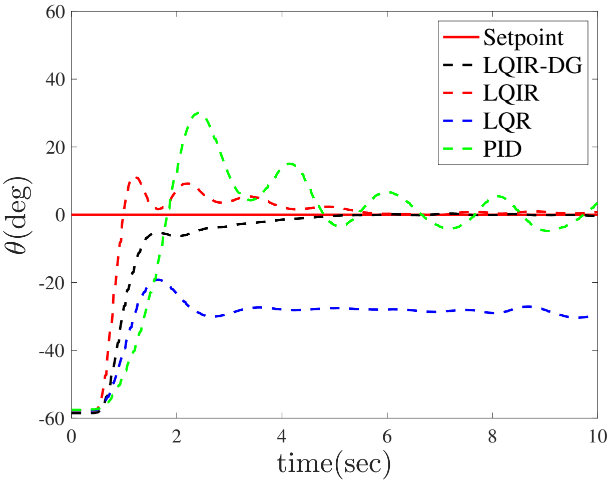

(b)

Figure 14: The performance of the LQIR-DG controller by adding weight to each of the roll and pitch axes in the three-degree-of-freedom coupling mode (a) Comparison of the roll angle with the actual value (b) Comparison of the pitch angle with the actual value (c) Comparison of the yaw angle with the actual value

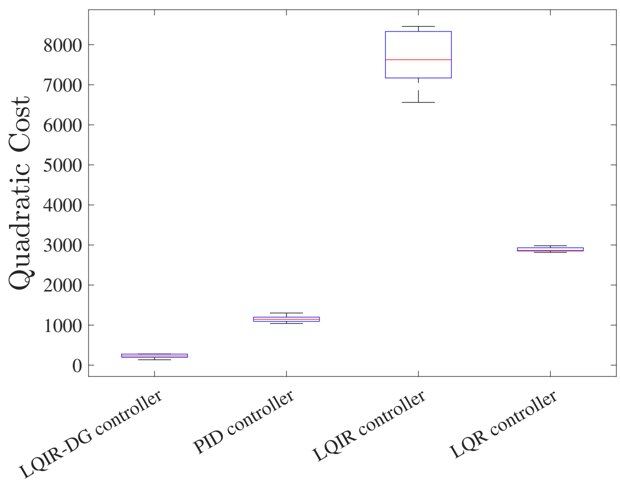

Figure 15: Comparison of the LQIR-DG to the PID quadratic cost function

6. Conclusion

This study presented the implementation and evaluation of a linear quadratic with integral action based on the differential game theory, named LQIR-DG, for level attitude control in an experimental setup of a quadrotor. The proposed controller structure required the linearization of an accurate model of the quadrotor in the state-space form and the estimation of the model parameters. The design of the LQIR-DG controller involved two players for each of the quadrotor's roll, pitch, and yaw channels. The first player optimized the control command for each channel based on the mini-maximization of a quadratic criterion, while the second player generated the worst disturbances. The evaluation of the LQIR-DG method was conducted in level flight and compared to the LQR controller. The results demonstrated the successful performance of the LQIR-DG method in level flight of the attitude control and tracking square wave, disturbance rejection, and model uncertainty in the actual plant.

References

[1] M. F. Fathoni, S. Lee, Y. Kim, K.-I. Kim, K. H. Kim, Development of multi-quadrotor simulator based on real-time hypervisor systems, Drones 5 (3). doi:10.3390/drones5030059.
URL https://www.mdpi.com/2504-446X/5/3/59

[2] H. Nobahari, A. Sharifi, A hybridization of extended kalman filter and ant colony optimization for state estimation of nonlinear systems, Applied Soft Computing 74. doi:10.1016/j.asoc.2018.10.010.

[3] H. Bolandi, M. Rezaei, R. Mohsenipour, H. Nemati, S. Smailzadeh, Attitude control of a quadrotor with optimized pid controller, Intelligent Control and Automation 04 (2013) 342–349. doi:10.4236/ica.2013.43040.

[4] A. Abdul Salam, I. Ibraheem, Nonlinear pid controller design for a 6-dof uav quadrotor system, Engineering Science and Technology, an International Journal 22. doi:10.1016/j.jestch.2019.02.005.

[5] Y. Bouzid, M. Zareb, H. Siguerdidjane, M. Guiatni, Boosting a Reference Model-Based Controller Using Active Disturbance Rejection Principle for 3D Trajectory Tracking of Quadrotors: Experimental Validation, Journal of Intelligent and Robotic Systems 100 (2) (2020) 597–614. doi:10.1007/s10846-020-01182-4.
URL https://hal.univ-grenoble-alpes.fr/hal-02543214

[6] Z. Wang, D. Huang, T. Huang, N. Qin, Active disturbance rejection control for a quadrotor uav, in: 2020 IEEE 9th Data Driven Control and Learning Systems Conference (DDCLS), 2020, pp. 1–5. doi:10.1109/DDCLS49620.2020.9275226.

[7] C. Nicol, C. Macnab, A. Ramirez-Serrano, Robust neural network control of a quadrotor helicopter, in: 2008 Canadian Conference on Electrical and Computer Engineering, 2008, pp. 001233–001238. doi:10.1109/CCECE.2008.4564736.

[8] P. Ghiglino, J. L. Forshaw, V. J. Lappas, Online PID Self-Tuning using an Evolutionary Swarm Algorithm with Experimental Quadrotor Flight Results. arXiv:https://arc.aiaa.org/doi/pdf/10.2514/6.2013-5098, doi:10.2514/6.2013-5098.
URL https://arc.aiaa.org/doi/abs/10.2514/6.2013-5098

[9] L. V. Nguyen, M. D. Phung, Q. P. Ha, Iterative learning sliding mode control for uav trajectory tracking, Electronics 10 (20). doi:10.3390/electronics10202474.
URL https://www.mdpi.com/2079-9292/10/20/2474

[10] C.-H. Pi, W.-Y. Ye, S. Cheng, Robust quadrotor control through reinforcement learning with disturbance compensation, Applied Sciences 11 (7). doi:10.3390/app11073257.
URL https://www.mdpi.com/2076-3417/11/7/3257

[11] K. Liu, R. Wang, S. Dong, X. Wang, Adaptive fuzzy finite-time attitude controller design for quadrotor uav with external disturbances and uncertain dynamics, in: 2022 8th International Conference on Control, Automation and Robotics (ICCAR), 2022, pp. 363–368. doi:10.1109/ICCAR55106.2022.9782598.

[12] K. Chara, A. Yassine, F. Srairi, K. Mokhtari, A robust synergetic controller for quadrotor obstacle avoidance using bézier curve versus b-spline trajectory generation, Intelligent Service Robotics 15. doi:10.1007/s11370-021-00408-0.

[13] H. Wang, M. Chen, Sliding mode attitude control for a quadrotor micro unmanned aircraft vehicle using disturbance observer, in: Proceedings of 2014 IEEE Chinese Guidance, Navigation and Control Conference, 2014, pp. 568–573. doi:10.1109/CGNCC.2014.7007285.

[14] A. Aboudonia, A. El-Badawy, R. Rashad, Disturbance observer-based feedback linearization control of an unmanned quadrotor helicopter, Proceedings of the Institution of Mechanical Engineers Part I Journal of Systems and Control Engineering 230. doi:10.1177/0959651816656951.

[15] A. T. Azar, F. E. Serrano, A. Koubaa, N. A. Kamal, Backstepping h-infinity control of unmanned aerial vehicles with time varying disturbances, in: 2020 First International Conference of Smart Systems and Emerging Technologies (SMARTTECH), 2020, pp. 243–248. doi:10.1109/SMART-TECH49988.2020.00061.

[16] A. Hamza, A. Mohamed, A. El-Badawy, Robust h-infinity control for a quadrotor uav, 2022. doi:10.2514/6.2022-2033.

[17] W. Dean, B. Ranganathan, I. Penskiy, S. Bergbreiter, J. Humbert, Robust Gust Rejection on a Micro-air Vehicle Using Bio-inspired Sensing, 2017, pp. 351–362.

[18] E. Barzanooni, K. Salahshoor, A. Khaki Sedigh, Attitude flight control system design of uav using lqg ltr multivariable control with noise and disturbance, in: 2015 3rd RSI International Conference on Robotics and Mechatronics (ICROM), 2015, pp. 188–193. doi:10.1109/ICRoM.2015.7367782.

[19] Z. Shulong, A. Honglei, Z. Daibing, S. Lincheng, A new feedback linearization lqr control for attitude of quadrotor, in: 2014 13th International Conference on Control Automation Robotics and Vision (ICARCV), 2014, pp. 1593–1597. doi:10.1109/ICARCV.2014.7064553.

[20] Z. Zwierzewicz, On the ship course-keeping control system design by using robust and adaptive control, in: 2014 19th International Conference on Methods and Models in Automation and Robotics (MMAR), 2014, pp. 189–194. doi:10.1109/MMAR.2014.6957349.

[21] Y. Li, L. Guo, Towards a theory of stochastic adaptive differential games, in: 2011 50th IEEE Conference on Decision and Control and European Control Conference, 2011, pp. 5041–5046. doi:10.1109/CDC.2011.6160768.

[22] S. Bouabdallah, R. Siegwart, Full control of a quadrotor, in: 2007 IEEE/RSJ International Conference on Intelligent Robots and Systems, 2007, pp. 153–158. doi:10.1109/IROS.2007.4399042.

[23] S. Bouabdallah, Design and control of quadrotors with application to autonomous flyingdoi:10.5075/epfl-thesis-3727.

[24] J. Eriksson, Optimization and regularization of nonlinear least squares problems.

[25] J. Engwerda, Linear quadratic games: An overview, Workingpaper, Macroeconomics, subsequently published in Advances in Dynamic Games and their Applications (book), 2009 Pagination: 32 (2006).